J Fluoresc (2015) 25:1567–1575
DOI 10.1007/s10895-015-1665-3

SHORT COMMUNICATION

A Note on the use of Steady–State Fluorescence Quenching to Quantify Nanoparticle–Protein Interactions

Alioscka A. Sousa [1]

Received: 9 June 2015 / Accepted: 14 September 2015 / Published online: 26 September 2015

Abstract Steady–state fluorescence quenching is a commonly used technique to investigate the interactions between proteins and nanoparticles, providing quantitative information on binding affinity, stoichiometry and cooperativity. However, a failure to account for the limitations and pitfalls of the methodology can lead to significant errors in data analysis and interpretation. Thus, in this communication we first draw attention to a few common pitfalls in the use of fluorescence quenching to study nanoparticle–protein interactions. For example, we discuss a frequent mistake in the use of the Hill equation to determine cooperativity. We also test using both simulated and experimental data the application of a model–independent method of analysis to generate true thermodynamic nanoparticle–protein binding isotherms. This model–free approach allows for a quantitative description of the interactions independent of assumptions about the nature of the binding process [Bujalowski W, Lohman TM (1987) Biochemistry 26: 3099; Schwarz G (2000) Biophys. Chem. 86: 119].

Keywords Fluorescence quenching · Spectroscopic titration · Hill equation · Gold nanoparticles · Protein adsorption

Electronic supplementary material The online version of this article (doi:10.1007/s10895-015-1665-3) contains supplementary material, which is available to authorized users.

✉ Alioscka A. Sousa
alioscka.bioq@gmail.com

[1] Department of Biochemistry, Federal University of São Paulo, São Paulo, SP 04044, Brazil

Introduction

Understanding the molecular interactions of proteins with nanoparticles is required for the rational design and application of nanoparticles in biomedicine [1–4]. Steady–state fluorescence quenching is a simple–to–use technique that has been traditionally utilized to quantify nanoparticle–protein interactions in terms of binding affinity, stoichiometry and cooperativity, thus providing important insights into the nature of the binding process [5–12].

The application of fluorescence quenching to characterize nanoparticle–protein complexation follows the same basic principles underlying the use of this technique to measure protein–ligand binding, protein–protein interactions and nucleic acid–protein interactions [13–15]. However, despite the fact that fluorescence quenching is such an established method to investigate binding in general, it has been shown recently that basic errors in experimental design, data analysis and interpretation have become widespread [16–23]. In fact, we have noticed similar problems in the application of the fluorescence methodology to study nanoparticle–protein interactions.

Thus, in this communication we first draw attention to some critical errors that can occur in the quantification of protein binding to nanoparticles using fluorescence quenching. Using simulated data, we also illustrate the applicability of the Lohman–Bujalowski's and Schwarz's methodology to generate true thermodynamic nanoparticle–protein binding isotherms [17, 24–26]. We finally test, for the first time to our knowledge, the application of this model–free approach to quantify the association of a model protein, α–chymotrypsin, to a gold nanoparticle.

Basics of Fluorescence Quenching in the Study of Nanoparticle–Protein Interactions

Initial Definitions

Here we consider the case of protein binding to gold nanoparticles (AuNPs). We assume the AuNPs are spherical, monodisperse and coated uniformly with an organic passivating layer. It is also assumed that nanoparticle–protein complexes exist in thermodynamic equilibrium with free proteins and nanoparticles, which excludes cases of adsorption where the protein is denatured irreversibly.

We consider the typical case where n proteins P can bind a single nanoparticle N. The proteins have a single interaction site to the AuNPs so that aggregation does not occur. We then have the equilibrium equation:

$$nP + N <=> P_nN \tag{1}$$

The proteins saturate the nanoparticle surface sequentially and not in a single step as may be implied by Eq. 1, so the molar concentration of bound proteins, $[P]_b$, is given by:

$$[P]_b = \sum i[P_iN] \tag{2}$$

where $[P_iN]$ is the molar concentration of the individual nanoparticle–protein species P_iN, and the sum goes from i=1 to n.

The molar ratio, r, of bound protein to total nanoparticle is then given by:

$$r = \frac{[P]_b}{[N]_t} = \frac{\sum i[P_iN]}{[N]_f + \sum [P_iN]} \tag{3}$$

where $[N]_t$ and $[N]_f$ are the molar concentrations of total and free nanoparticles, respectively. Hereafter we will refer to r as the binding or packing density [24].

Eq. 3 can be transformed and be written as a function of the free concentration of ligand, $[P]_f$ (the subscript f below was removed for clarity), leading to the *Adair equation* [27, 28]:

$$r = \frac{\frac{[P]}{Kd_1} + \frac{2[P]^2}{Kd_1Kd_2} + \ldots + \frac{n[P]^n}{Kd_1Kd_2\ldots Kd_n}}{1 + \frac{[P]}{Kd_1} + \frac{[P]^2}{Kd_1Kd_2} + \ldots + \frac{[P]^n}{Kd_1Kd_2\ldots Kd_n}} \tag{4}$$

where Kd_i (i=1…n) are the macroscopic dissociation constants for each binding step i.

When the binding of a single protein to the nanoparticle surface does not influence subsequent binding events (independent binding model), then the individual values of Kd_i are related to the microscopic dissociation constant Kd according to

$$Kd_i = Kd \times i \Big/ (n + 1 - i) \tag{5}$$

In this case, Eq. 4 reduces to the Langmuir isotherm [27]:

$$r = \frac{n[P]_f}{[P]_f + Kd} \tag{6}$$

The Adair equation describes a general case where the individual macroscopic dissociation constants can assume any value. In the case of positive (negative) cooperativity for example, successive values of Kd_i will be smaller (larger) than those calculated from Eq. 5.

Fluorescence Signal

Here we assume the standard case where the fluorescence signal originates from the proteins via their aromatic amino acids. The total protein concentration is then kept constant in a cuvette while the total concentration of AuNPs is incremented gradually by titration. This titration scheme is known as "reverse", since the concentration of the ligand is fixed while the concentration of the "receptor", i.e., the species having the multiple binding sites (AuNPs), is varied.

Upon complexation, AuNPs most typically attenuate the emitted protein fluorescence by Förster resonance energy transfer (FRET), with the extent of quenching largely depending on the distance between the aromatic residues and the nanoparticle surface. Protein conformational changes taking place upon binding can also affect the quantum yield of the intrinsic fluorophores, leading to a further signal change.

Most typically, the measured fluorescence signal F is assumed to equal $F=\phi_f[P]_f+\phi_b[P]_b$, where ϕ_f and ϕ_b are the molar fluorescence of the proteins in the free and bound states, respectively. However, F is more correctly represented by

$$F = \phi_f[P]_f + \sum \phi_i \times i[P_iN] \tag{7}$$

Eq. 7 describes a generic situation where the molar fluorescence of the bound protein is not necessarily a constant, but instead it can depend on the degree of binding. For example, the possible formation of protein–protein contacts at the nanoparticle surface at high packing density could presumably stabilize the bound proteins in a specific conformation, thus leading to a unique value of ϕ_i.

Analysis Equations and Pitfalls

There are a number of model equations that can be applied to quantitatively describe fluorescence quenching data. However, substantial errors can occur if the analysis equations

are used inappropriately. For example, some equations are expressed as a function of the free ligand concentration, which is sometimes erroneously approximated by the known total ligand concentration. In addition, quenching data need to be accurately corrected for the inner–filter effect before any modeling can be attempted [29, 30]. These and other common sources of error have been critically discussed by van de Weert, Stella and others in recent years, mostly in the context of ligand binding to proteins [16, 18–20]. Next we will underscore some of the limitations and pitfalls of the fluorescence methodology as specifically applied to the study of nanoparticle–protein interactions.

Use of the Stern–Volmer equation is a common approach to analyze spectroscopic titration data [29]. However, this method of analysis is limited in that it does not provide information on binding stoichiometry and cooperativity. Therefore, we will not discuss the Stern–Volmer method further.

The Hill equation offers another very popular means for quantifying fluorescence quenching data [8, 10, 12]:

$$\frac{F_0-F}{F_0-F_{max}}=\frac{[N]_f{}^h}{[N]_f{}^h+Kd^h} \tag{8}$$

where F_0 is the initial protein fluorescence, F_{max} is the fluorescence signal at saturation, and h is the Hill coefficient. The first challenge in the application of the Hill equation is that it is expressed as a function of the free nanoparticle concentration, which cannot always be approximated by $[N]_t$. In addition, there is a major pitfall associated with the use of Eq. 8, which to our knowledge has not yet been described. Eq. 8 is written as a function of $[N]_f$ (and not $[P]_f$) since the nanoparticles are the species being titrated. However, it is impossible to derive this equation starting from Eq. 1. To see this, we first write the basic relations $Kd = [N]_f[P]_f^n/[P_nN]$ and $[P]_f=[P]_t-[P_nN]$. Substituting the latter into the former to remove $[P]_f$ leads to a term raised to the power of n that cannot be simplified further. In other words, this problem arises because the titration scheme is reverse, as defined previously. It then actually follows that application of Eq. 8 to quantify nanoparticle–protein quenching data obtained by reverse titration, as commonly done, will lead to an inverse relationship between h and cooperativity: i.e., h will be larger and smaller than 1 for negative and positive cooperativity, respectively.

Interestingly, Nienhaus and co–workers have reported the synthesis of a fluorescent AuNP whose near–infrared fluorescence signal increases upon protein binding [31]. Therefore, they were able to use a direct titration scheme in their protein binding studies, in which case the quenching data could be fitted to Eq. 8 with $[N]_f$ replaced by $[P]_f$.

If it is known that protein association to nanoparticles is noncooperative, then the following equation, expressed as a function of $[N]_t$, can be used for an accurate determination of n and Kd [32]:

$$\frac{F_0-F}{F_0-F_{max}}=\frac{[P]_t+n[N]_t+Kd-\sqrt{\left([P]_t+n[N]_t+Kd\right)^2-4n[P]_t[N]_t}}{2[P]_t} \tag{9}$$

However, it is typically never known a priori whether the binding is noncooperative.

Finally, these standard analysis methods are strictly applicable only when there is a single value of ϕ_b that is independent of packing density. Data analysis may be further complicated in case the molar fluorescence of the bound proteins varies significantly with the degree of binding.

Lohman-Bujalowski's and Schwarz's Model-Independent (General) Method of Analysis

The model–independent method of analysis allows the conversion of a set of fluorescence quenching curves into true thermodynamic binding isotherms, which by definition embody the unique relationship between the binding density r and the free ligand concentration (here $[P]_f$) [17, 22, 24–26]. To our knowledge, this general method has not yet been applied to study nanoparticle–protein interactions. Thus, for completeness we will provide next a brief description of the method.

First we write the general relationship: $[P]_t=[P]_f+r[N]_t$. The general method of analysis consists in finding several pairs of values $[P]_t$ and $[N]_t$ resulting in the same degree of binding. A plot of $[P]_t$ vs. $[N]_t$ then gives a straight line whose slope and ordinate intercept provide r and $[P]_f$, respectively. The process is repeated until sufficient values of r and $[P]_f$ are obtained to construct a binding isotherm.

In order to find the appropriate $[P]_t$ and $[N]_t$, reverse titration curves obtained for several different $[P]_t$ are first each transformed according to the equation

$$F'=\frac{(F_0-F)}{F_0}\left(\frac{[P]_t}{[N]_t}\right) \tag{10}$$

and plotted as a function of $\log([N]_t)$.

It can be also shown that

$$F'=\sum\frac{(\phi_f-\phi_i)}{\phi_f}r_i \tag{11}$$

where $r_i=i[P_iN]/[N]_t$.

It can be seen from Eq. 11 that a given F' defines a unique value of $r=\sum r_i$ and, by definition, a unique $[P]_f$ as well. Thus, values of $[P]_t$ and $[N]_t$ resulting in the same degree of binding can be found by drawing horizontal lines across the plots F' *vs.* $\log([N]_t)$ (Eq. 10) and finding the pairs $([P]_t,[N]_t)$ at the intersection points.

The general method of analysis can also provide information on how the molar fluorescence of bound proteins changes

with binding density [26]. A plot of F'/r *vs*.r will give a horizontal line in case ϕ_i assumes a single value for all i (in which case $\phi_i=\phi_b$), or a sloped line in case of a varying ϕ_i. This information, in turn, can offer insights into whether the conformation and/or orientation of the bound proteins are influenced by the degree of packing.

We finally point out that a thermodynamic binding isotherm can be constructed from only a single spectroscopic titration curve provided the molar fluorescence of the bound proteins assumes a constant value ϕ_b. Unfortunately, this is typically not known a priori. Additional details on this topic can be found in the works by Lohman and Bujalowski [17, 24, 25].

Materials and Methods

Simulated Binding Models

Fluorescence quenching data was simulated with the program Dynafit® [33]. The parameters of the simulated models are summarized in Table 1, and a general script is provided in the Supplementary Information. For each model, titration curves were simulated for six successive protein concentrations: 0.6, 0.9, 1.35, 2.03, 3.04, 4.56 μM. The maximum titrated AuNP concentration was 2 μM.

Reagents and Buffers

Ultrasmall and uniform AuNPs were synthesized and characterized as described previously [34, 35]. The AuNPs had a core diameter of about 2 nm and were coated with a monolayer of 4–mercaptobenzoic acid molecules. The AuNPs were negatively charged, with a zeta potential of −18.4 mV in phosphate buffer supplemented with 0.1M NaF (pH = 7.2). AuNPs of similar size but coated with glutathione monoethyl ester were used as a stealth, non–interacting nanoparticle control to validate the inner–filter correction procedure (see text for details). High purity (sequencing–grade) α–chymotrypsin was purchased from Sigma–Aldrich. The concentration of AuNPs in solution was estimated from absorbance measurements assuming an extinction coefficient of $4.34\text{x}10^5\ M^{-1}cm^{-1}$ at 510 nm [34], while the concentration of α–chymotrypsin was determined with the Bradford assay. Phosphate buffers (10 mM; pH 7.4) supplemented with either 10 or 150 mM NaCl were used in the titration experiments.

Fluorescence Measurements

Fluorescence measurements were performed on a Shimadzu spectrofluorometer model RF-5301PC at 20 °C. A fixed amount of α–chymotrypsin was loaded into a quartz cuvette and its fluorescence signal measured following each titration from a concentrated stock solution of AuNPs. The excitation wavelength was 280 nm. Titration curves were obtained at the protein concentrations of 0.8, 1, 1.25, 1.56, 1.95, 2.44, 3.05, 3.81, 4.77 μM. The binding experiments were performed in buffer supplemented with 10 mM NaCl. Control experiments using the stealth AuNP were performed in 150 mM NaCl. Tryptophan correction curves were obtained following identical procedures, except that tryptophan concentrations of 4, 8 and 16 μM were used.

Results and Discussion

Analysis of Simulated Data with the General Method of Analysis

Analytical models such as those described by Eqs. 4 and 6 (representing cooperativity and independent binding,

Table 1 Nanoparticle–protein interaction models employed in the simulations

Model *	Type	Kd_i	ϕ_i
1	Independent binding and constant ϕ_i	$Kd_i = \frac{iKd}{n+1-i}$	ϕ_i=0
2	Independent binding and varying ϕ_i	$Kd_i = \frac{iKd}{n+1-i}$	$\phi_i = 0\ (i = 1,2,3)$ $\phi_i = 0.2\ (i = 4,5)$
3	Negative cooperativity§ and constant ϕ_i	$Kd_i = \frac{1}{\alpha^{(i-1)}} \frac{iKd}{n+1-i}$	ϕ_i=0
4	Negative cooperativity and varying ϕ_i	$Kd_i = \frac{1}{\alpha^{(i-1)}} \frac{iKd}{n+1-i}$	$\phi_i = 0\ (i = 1,2,3)$ $\phi_i = 0.2\ (i = 4,5)$

*For all models: n=5, Kd = 100 nM, ϕ_f=1

§ Equation adapted from the Pauling model of cooperativity [27]. Negative cooperativity can be simulated by assigning $\alpha < 1$ (here $\alpha = 0.7$)

respectively) are not suitable for simulations because they are expressed as a function of $[P]_f$, while ideally we would like to simulate titration curves as a function of $[N]_t$ to mimic real data. Furthermore, these analytical models do not incorporate the possibility of a unique ϕ_i for each species P_iN (Eq. 7). Thus, simulations were performed with the program Dynafit®, allowing for total flexibility in how different binding models could be set up.

Fluorescence quenching data was simulated according to four distinct binding models (Table 1). Figure 1 shows that the set of titration curves was "well-behaved" for Model 1: the curves appeared shifted to the right with increasing $[P]_t$, but maintained the same curvature irrespective of $[P]_t$. On the other hand, Models 2–4, representing complex binding equilibria, resulted in titration curves whose curvature decreased with $[P]_t$ (this effect is particularly clear with Model 4). Analysis of any *single* spectroscopic titration curve is not able to provide all model parameters (n, Kd, h and ϕ) or even to discriminate the nature of the binding process itself (independent binding vs. cooperativity). Much more information can be gained by analyzing the whole set of multiple titration curves.

The set of curves in Fig. 1 was therefore quantitatively evaluated with the model–independent method of analysis to extract all parameters n, Kd, h and ϕ. The calculated thermodynamic binding isotherms are displayed in Fig. 2. These isotherms were modeled with the following Hill equation

$$r = n\frac{[P]_f{}^h}{[P]_f{}^h + Kd^h} \tag{12}$$

yielding reasonably accurate estimates for n, Kd and h (see Fig. 2). The plots F'/r *vs*.r (Fig. 2, insets) also revealed the correct trends. Specifically, for Models 1 and 3, the plots resulted in a horizontal line crossing the ordinate at 1, thus indicating that the molar fluorescence of the bound proteins was constant with r and equal to 0 (i.e., $\phi_i=\phi_b=0$). Conversely, for Models 2 and 4, F'/r *vs*.r showed that $\phi_i=0$ and $\phi_i>0$ for low and high values of the binding density r, respectively.

In theory, it is possible to improve the above analysis even further by including additional points in the binding isotherms. This would require increasing the ranges of $[P]_t$ and $[N]_t$ beyond 0.6–4.56 μM and 2.0 μM, respectively. In practice, other factors may limit the use of the general method of analysis, such as the inner–filter effect. Thus, we will evaluate next the applicability of the general method to quantify the association of a model protein, α–chymotrypsin, to a AuNP. First, however, we will explain how the inner–filter effect could be accurately corrected for in our experiments.

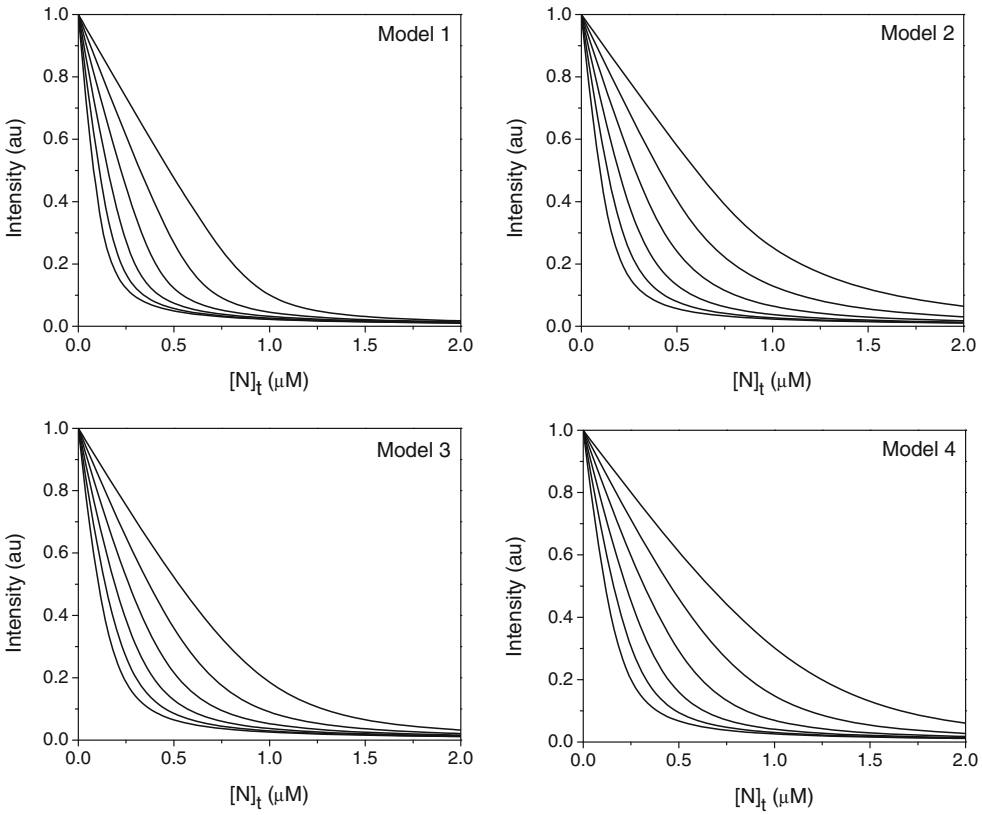

Fig. 1 Simulated fluorescence quenching data for α–chymotrypsin binding to a gold nanoparticle. Simulations were performed using the program Dynafit® assuming four distinct interaction models as specified in Table 1. Titration curves were simulated for six successive protein concentrations (from left to right): 0.6, 0.9, 1.35, 2.03, 3.04, 4.56 μM

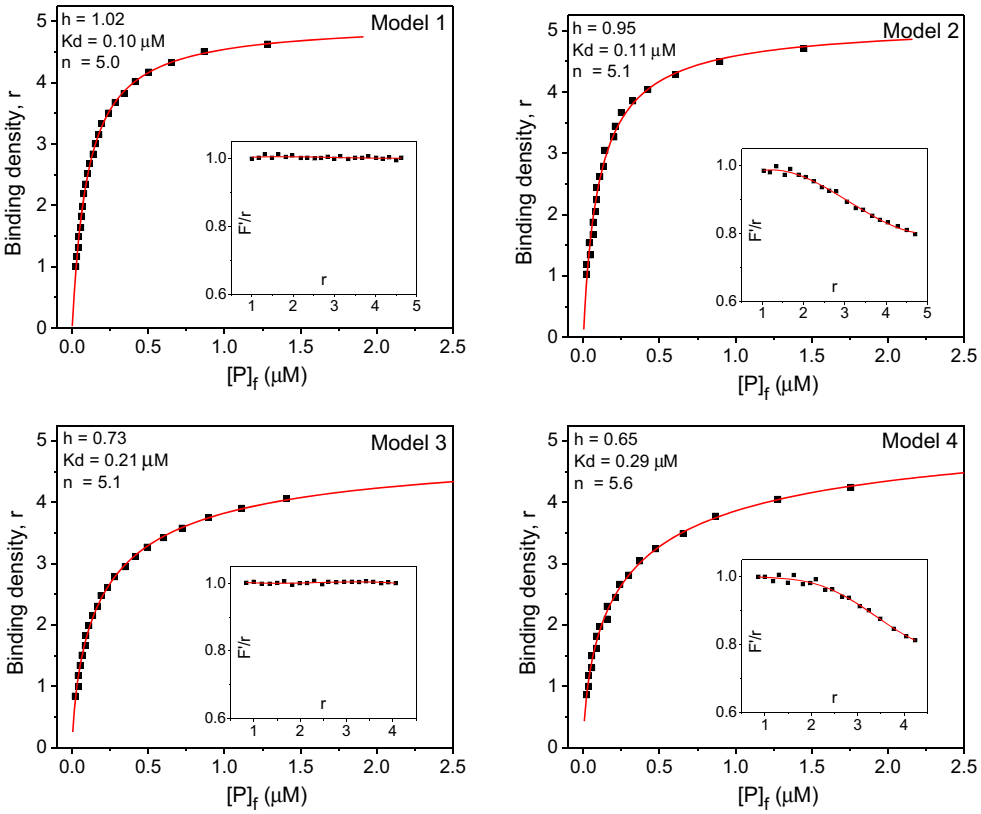

Fig. 2 Binding isotherms constructed by applying the general method of analysis to the simulated data in Fig. 1. The isotherms were modeled with the Hill equation (Eq. 12) yielding the binding parameters *n*, *Kd* and *h* displayed on each plot. The solid lines are fits to the data points. Insets show the correct trends for the molar fluorescence of bound proteins (solid lines are guide to the eye). See text for details

Correction of the Inner–Filter Effect

Fluorescence quenching measurements are complicated by an inner–filter effect from the AuNPs, which relates to the strong light attenuation by the AuNPs at both the excitation and emission wavelengths [36, 37]. We generated correction curves by titrating the AuNPs into a solution of the amino acid tryptophan, where the observed signal decrease was due exclusively to the inner–filter effect (Fig. 3a). A corrected α–chymotrypsin fluorescence quenching curve could then be calculated by dividing the uncorrected data by the tryptophan correction curve (Fig. 3a). We established the validity and accuracy of this correction approach according to the following control experiments. First, we checked that tryptophan did not bind to the AuNPs by performing the titrations at different tryptophan concentrations and in phosphate buffers of different ionic strengths (10 and 150 mM NaCl). All "quenching" curves were superimposed on each other, therefore indicating that the tryptophan signal decrease was due uniquely to the inner–filter effect (data not shown). Second, the accuracy of the correction was confirmed by applying it to fluorescence data for α–chymotrypsin obtained in the absence of binding (Fig. 3b). This was accomplished by using a stealth, non–interacting AuNP in the titrations. After correction, the resultant quenching curve became a horizontal line crossing the ordinate at 1, in agreement with the known lack of interaction between α–chymotrypsin and the nanoparticles.

Analysis of α–Chymotrypsin Binding to an Ultrasmall (2 nm) AuNP

Figure 4a shows the set of titration curves for α–chymotrypsin. First, a simple visual inspection reveals the curves are not "well–behaved" as defined previously, therefore indicating complexities in binding. To see this more clearly, we also attempted to perform a *global fit* of the experimental data to Eq. 9 (Fig. 4b). The bad quality of the fit confirmed that α–chymotrypsin association with the AuNPs could not be described by a simple model which assumed independent binding events and a constant ϕ_b.

The set of titration curves were then processed according to the general method of analysis (Fig. 4c, d) resulting in the thermodynamic binding isotherm depicted in Fig. 4e. Fitting Eq. 12 to the isotherm yielded Kd = 283 nM, n = 6.1 and h = 0.57. The Hill coefficient of 0.57 specifies that α–chymotrypsin binding is anti-cooperative, i.e., binding becomes progressively more difficult as the nanoparticle surface gets populated with proteins. This would be consistent with an association model where the first α–chymotrypsin proteins bind unhindered to the still vacant AuNP surface. In contrast, the last proteins to bind would need presumably to negotiate their way towards the

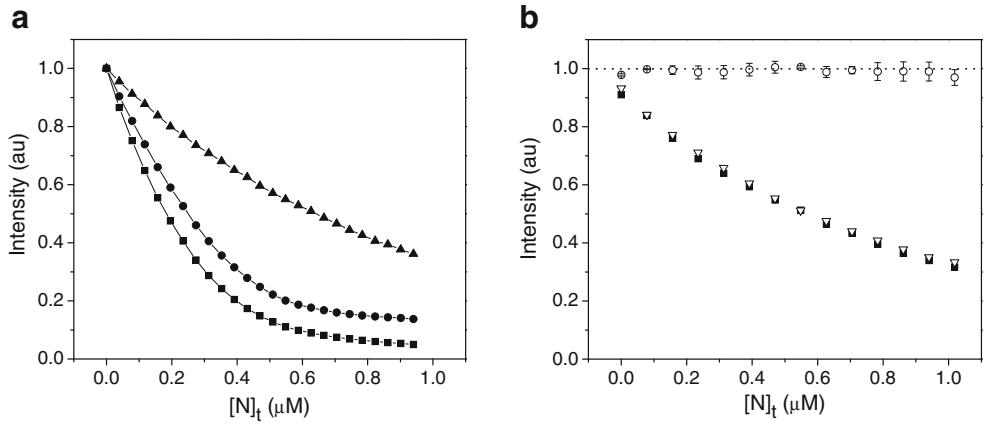

Fig. 3 Correction of the inner–filter effect from AuNPs. **a** Example of corrected α–chymotrypsin fluorescence quenching curve (circles) calculated by dividing the uncorrected data for α–chymotrypsin (squares) by the tryptophan correction curve (triangles). **b** The accuracy of the inner–filter correction approach was tested by applying it to AuNP–protein fluorescence quenching data obtained in the absence of binding. Corrected α–chymotrypsin quenching curve (circles) obtained by dividing uncorrected data (squares) by tryptophan correction curve (triangles) resulted in a horizontal line crossing the ordinate at 1, in agreement with the known lack of interaction between α–chymotrypsin and the nanoparticles

nanoparticle surface due to steric repulsion from the protein layer already formed. Further analysis also showed that the molar fluorescence of the bound proteins changed slightly with *r* (Fig. 4f), suggesting that α–chymotrypsin may adopt different conformations on the AuNP surface depending on the packing density (at a high packing density the conformation would be such as to produce greater net quenching).

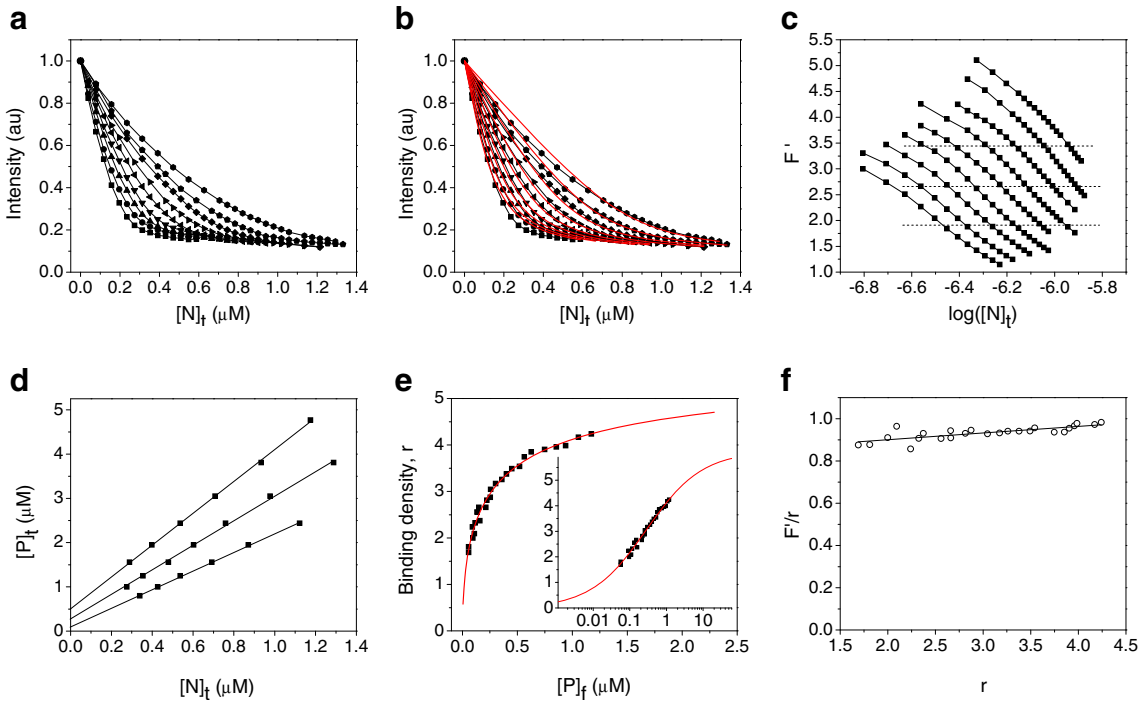

Fig. 4 Characterization of α–chymotrypsin binding to an ultrasmall AuNP by the model– independent method of analysis. **a** Set of multiple titration curves obtained for nine successive protein concentrations (from left to right): 0.8, 1, 1.25, 1.56, 1.95, 2.44, 3.05, 3.81, 4.77 μM. **b** Global fit of titration curves from a) to Eq. 9 (refer to online version for color). Bad quality of the fit shows the data cannot be described by a simple model which assumes independent binding events and a constant ϕ_b. **c** Titration data transformed according to Eq. 10. The intersection between horizontal lines and the titration curves defines a set of values $[P]_f$ and $[N]_f$ resulting in the same degree of binding. **d** Plotting the values of $[P]_f$ and $[N]_f$ found from c) yields straight lines whose slope and ordinate intercept give *r* and $[P]_f$, respectively. **e** Resulting binding isotherm was fitted to the Hill equation (Eq. 12) yielding $Kd = 283$ nM, $n = 6.1$ and $h = 0.57$. **f** The molar fluorescence of bound α–chymotrypsin varied slightly with *r*, suggesting the protein may adopt different conformations on the AuNP surface depending on packing density

Conclusions

Here we have briefly underlined some of the pitfalls in the use of fluorescence quenching to investigate nanoparticle–protein interactions. If not properly recognized, these pitfalls can lead to substantial errors in the quantification of the interaction parameters. We have also illustrated the applicability of the Lohman–Bujalowski's and Schwarz's general method of analysis to quantify nanoparticle–protein binding using data simulated with the program Dynafit®. We finally tested this model–free approach in practice by characterizing the association of α–chymotrypsin with an ultrasmall AuNP. Importantly, the general method allowed for a quantitative description of the association process without the underlying assumptions that prevail in other standard methods of analysis. Despite these advantages, it should be clear that a complete and genuine picture of the association process can only emerge with the combination of multiple characterization techniques.

Acknowledgments This work was supported by the São Paulo Research Foundation (FAPESP grant # 2013/18481-5), São Paulo, Brazil, and by the National Council for Scientific and Technological Development (CNPq grant # 476784/2013-1), Brazil.

References

1. Treuel L, Nienhaus GU (2012) Toward a molecular understanding of nanoparticle–protein interactions. Biophys Rev 4:137–147
2. Cedervall T, Lynch I, Lindman S, Berggård T, Thulin E, Nilsson H, Dawson KA, Linse S (2007) Understanding the nanoparticle–protein corona using methods to quantify exchange rates and affinities of proteins for nanoparticles. Proc Natl Acad Sci U S A 104:2050–2055
3. Tonga GY, Saha K, Rotello VM (2014) 25th anniversary article: interfacing nanoparticles and biology: new strategies for biomedicine. Adv Mater 26:359–370
4. Pd P, Pelaz B, Zhang Q, Maffre P, Nienhaus GU, Parak WJ (2014) Protein corona formation around nanoparticles – from the past to the future. Mater Horiz 1:301–313
5. Xiao Q, Huang S, Su W, Li P, Ma J, Luo F, Chen J, Liu Y (2013) Systematically investigations of conformation and thermodynamics of HSA adsorbed to different sizes of CdTe quantum dots. Colloids Surf B: Biointerfaces 102:76–82
6. Liang J, Cheng Y, Han H (2008) Study on the interaction between bovine serum albumin and CdTe quantum dots with spectroscopic techniques. J Mol Struct 892:116–120
7. Jhonsi MA, Kathiravan A, Renganathan R (2009) Spectroscopic studies on the interaction of colloidal capped CdS nanoparticles with bovine serum albumin. Colloids Surf B: Biointerfaces 72:167–172
8. Shang L, Dörlich RM, Trouillet V, Bruns M, Nienhaus GU (2012) Ultrasmall fluorescent silver nanoclusters: protein adsorption and its effects on cellular responses. Nano Res 5:531–542
9. Shang L, Yang L, Seiter J, Heinle M, Brenner-Weiss G, Gerthsen D, Nienhaus GU (2014) Nanoparticles interacting with proteins and cells: a systematic study of protein surface charge effects. Adv Mater Interfaces 1:2014
10. Boulos SP, Davis TA, Yang JA, Lohse SE, Alkilany AM, Holland LA, Murphy CJ (2013) Nanoparticle − protein interactions: a thermodynamic and kinetic study of the adsorption of bovine serum albumin to gold nanoparticle surfaces. Langmuir 29:14984–14996
11. Yang JA, Johnson BJ, Wu S, Woods WS, George JM, Murphy CJ (2013) Study of wild-type α-synuclein binding and orientation on gold nanoparticles. Langmuir 29:4603–4615
12. Lacerda SHDP, Park JJ, Meuse C, Pristinski D, Becker ML, Karim A, Douglas JF (2010) Interaction of gold nanoparticles with common human blood proteins. ACSNano 4:365–379
13. Andrews AJ, Downing G, Brown K, Park Y-J, Luger1 K (2008) A thermodynamic model for Nap1-histone interactions. J Biol Chem 283:32412–32418
14. Carpenter ML, Oliver AW, Kneale GG (2001) Analysis of DNA-protein interactions by intrinsic fluorescence. Methods Mol Biol 148:491–502
15. Beckett D (2011) Measurement and analysis of equilibrium binding titrations: a beginner's guide. Methods Enzymol 488:1–16
16. Lissi E, Abuin E (2011) On the evaluation of the number of binding sites in proteins from steady state fluorescence measurements. J Fluoresc 21:1831–1833
17. Bujalowski W, Jezewska MJ (2014) Quantitative thermodynamic analyses of spectroscopic titration curves. J Mol Struct 1077:40–50
18. Mvd W (2010) Fluorescence quenching to study protein-ligand binding: common errors. J Fluoresc 20:625–629
19. Mvd W, Stella L (2011) Fluorescence quenching and ligand binding: a critical discussion of a popular methodology. J Mol Struct 998:144–150
20. Stella L, Mvd W, Burrows HD, Fausto R (2014) Fluorescence spectroscopy and binding: getting it right. J Mol Struct 1077:1–3
21. Grossweiner LI (2000) A note on the analysis of ligand binding by the 'double-logarithmic' plot. J Photochem Photobiol B: Biology 58:175–177
22. Lissi E, Calderon C, Campos A (2013) Evaluation of the number of binding sites in proteins from their intrinsic fluorescence: limitations and pitfalls. Photochem Photobiol 89:1413–1416
23. Stella L, Capodilupo AL, Bietti M (2008) A reassessment of the association between azulene and [60]fullerene. Possible pitfalls in the determination of binding constants through fluorescence spectroscopy. Chem Commun (39):4744–4746
24. Bujalowski W, Lohman TM (1987) A general method of analysis of ligand-macromolecule equilibria using a spectroscopic signal from the ligand to monitor binding. Application to Escherichia coli Single-Strand Binding Protein-Nucleic Acid Interactions. Biochemistry 26:3099–3106
25. Bujalowski W (2006) Thermodynamic and kinetic methods of analyses of protein − nucleic acid interactions. From Simpler to More Complex Systems. Biochemistry 106:556–606
26. Schwarz G (2000) A universal thermodynamic approach to analyze biomolecular binding experiments. Biophys Chem 86:119–129
27. Bisswanger H (2008) Multiple equilibria. In: Bisswanger H (ed) Enzyme kinetics: principles and methods, 2nd edn. Wiley-VCH Verlag GmbH & Co. KGaA, Weinheim, pp. 7–58
28. Adair GS (1925) The hemoglobin system. The Oxygen dissociation Curve of Haemoglobin. J Biol Chem 63:529–545
29. Zhang D, Nettles CB (2015) A generalized model on the effects of nanoparticles on fluorophore fluorescence in solution. J Phys Chem C 119:7941–7948
30. Credi A, Prodi L (2014) Inner filter effects and other traps in quantitative spectrofluorimetric measurements: origins and methods of correction. J Mol Struct 1077:30–39
31. Shang L, Brandholt S, Stockmar F, Trouillet V, Bruns M, Nienhaus GU (2012) Effect of protein adsorption on the fluorescence of ultrasmall gold nanoclusters. Small 8:661–665
32. Bunz UHF, Rotello VM (2010) Gold nanoparticle–fluorophore complexes: sensitive and discerning "noses" for biosystems sensing. Angew Chem Int Ed 39:3268–3279

33. Kuzmic P (1996) Program DYNAFIT for the analysis of enzyme kinetic data: application to HIV proteinase. Anal Biochem 237: 260–273
34. Ackerson CJ, Powell RD, Hainfeld JF (2010) Site-specific biomolecule labeling with gold clusters. Methods Enzymol 481:195–230
35. Sousa AA, Morgan JT, Brown PH, Adams A, Jayasekara MPS, Zhang G, Ackerson CJ, Kruhlak MJ, Leapman RD (2012) Synthesis, characterization, and direct intracellular imaging of ultrasmall and uniform glutathione-coated gold nanoparticles. Small 8:2277–2286
36. You C-C, Miranda OR, Gider B, Ghosh PS, Kim I-B, Erdogan B, Krovi SA, Bunz UHF, Rotello VM (2007) Detection and identification of proteins using nanoparticle–fluorescent polymer 'chemical nose' sensors. Nat Nanotech 2:318–323
37. Aguila A, Murray RW (2000) Monolayer-protected clusters with fluorescent dansyl. Langmuir 16:5949–5954